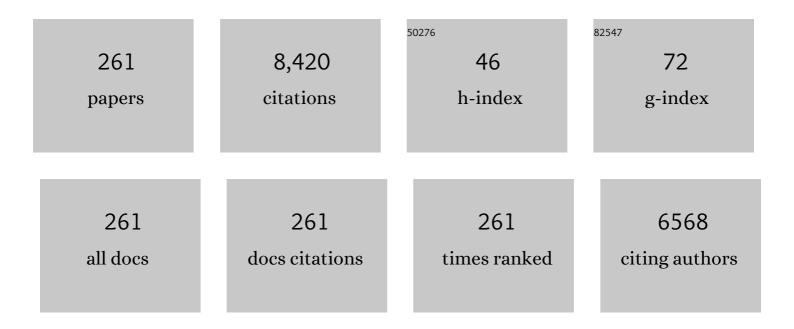
Hc Swart

List of Publications by Year in descending order

Source: https://exaly.com/author-pdf/11619602/publications.pdf Version: 2024-02-01



HC SWADT

#	Article	IF	CITATIONS
1	Photoluminescence, cathodoluminescence degradation and surface analysis of Gd2O3:Bi pulsed laser deposition thin films. Physica B: Condensed Matter, 2022, 631, 413618.	2.7	3
2	Charge compensated CaSr2(PO4)2:Sm3+, Li+/Na+/K+ phosphor: Luminescence and thermometric studies. Journal of Alloys and Compounds, 2022, 901, 163793.	5.5	22
3	Plasmonic Au nanoparticles embedded in glass: Study of TOF-SIMS, XPS and its enhanced antimicrobial activities. Journal of Alloys and Compounds, 2022, 909, 164789.	5.5	26
4	The morphology and downshifting luminescence of [CaY]F2 crystals doped with Ce3+/Eu3+/2+/Na+. Ceramics International, 2022, 48, 23657-23665.	4.8	1
5	Energy transfer mechanism in Eu3+ doped tin oxide nanophosphors for red solid state lighting. Journal of Luminescence, 2022, 250, 119085.	3.1	1
6	Upconversion process in BaY ₂ F ₈ :Yb ³⁺ ,Ho ³⁺ phosphor for optical thermometry. Luminescence, 2021, 36, 1847-1850.	2.9	8
7	Synthesis, surface and photoluminescence properties of Sm3+ doped α-Bi2O3. Journal of Alloys and Compounds, 2021, 854, 157221.	5.5	19
8	Luminescent behaviour of SrF2 and CaF2 crystals doped with Eu ions under different annealing temperatures. Journal of Alloys and Compounds, 2021, 858, 157741.	5.5	7
9	Color tuning of the Ba1.96Mg(PO4)2:0.04Eu2+ phosphor induced by the chemical unit co-substitution of the (BO3)3â^' anion group. Journal of Alloys and Compounds, 2021, 864, 158124.	5.5	8
10	Blue-emitting Ca3Mg3(PO4)4:Eu2+ phosphor: Study of electron-vibrational interaction in the 5d states of Eu2+ ions. Optical Materials, 2021, 114, 110959.	3.6	5
11	Synthesis and characterization of europium doped zinc selenide thin films prepared by photo-assisted chemical bath technique for luminescence application. Materials Chemistry and Physics, 2021, 262, 124303.	4.0	11
12	Fabrication of TiO2 nanofibers based sensors for enhanced CH4 performance induced by notable surface area and acid treatment. Vacuum, 2021, 187, 110102.	3.5	23
13	Structural and spectral studies of highly pure red-emitting Ca3B2O6:Eu3+ phosphors for white light emitting diodes. Journal of Alloys and Compounds, 2021, 869, 159363.	5.5	39
14	Structural, surface and luminescent properties of SrF2:Eu annealed thin films. Vacuum, 2021, 191, 110362.	3.5	8
15	Defects induced enhancement of antifungal activities of Zn doped CuO nanostructures. Applied Surface Science, 2021, 560, 150026.	6.1	50
16	Electron beam irradiation studies of ZnGa2O4:Mn2+ green phosphor. Vacuum, 2021, 192, 110447.	3.5	5
17	Evaluation of the effects of Au addition into ZnFe2O4 nanostructures on acetone detection capabilities. Materials Research Bulletin, 2021, 142, 111395.	5.2	15
18	Interface analysis of SrWO4:Er3+-Yb3+/Si thin films prepared by radio frequency magnetron sputtering for upconversion emission. Physica B: Condensed Matter, 2021, 623, 413349.	2.7	3

#	Article	IF	CITATIONS
19	The role of sulfate ions on distinctive defect emissions in ZnO:Ce3+ nanophosphors - A study on the application in color display systems. Journal of Luminescence, 2021, 240, 118462.	3.1	10
20	Study of photoluminescence and nonlinear optical behaviour of AgCu nanoparticles for nanophotonics. Nano Structures Nano Objects, 2021, 28, 100807.	3.5	11
21	Effect of oxygen partial pressure during pulsed laser deposition on the emission of Eu doped ZnO thin films. Physica B: Condensed Matter, 2020, 576, 411713.	2.7	17
22	Pulsed laser deposition of a ZnO:Eu3+ thin film: Study of the luminescence and surface state under electron beam irradiation. Applied Surface Science, 2020, 502, 144281.	6.1	21
23	Remarkable influence of alkaline earth ions on the enhancement of fluorescence from Eu3+ ion doped in sodium ortho-phosphate phosphors. Journal of Molecular Structure, 2020, 1203, 127375.	3.6	24
24	Characterization of the incorporated ZnO doped and co-doped with Ce3+ and Eu3+ nanophosphor powders into PVC polymer matrix. Journal of Molecular Structure, 2020, 1202, 127339.	3.6	17
25	Gas sensors based on CeO2 nanoparticles prepared by chemical precipitation method and their temperature-dependent selectivity towards H2S and NO2 gases. Applied Surface Science, 2020, 505, 144356.	6.1	67
26	Synthesis of silver incorporated lithium doped zinc oxide nanocomposites for in-vitro biorational evaluation of Candiasis and Cryptococcosis. Applied Surface Science, 2020, 506, 144800.	6.1	1
27	Effect of hydrazine hydrate as complexing agent in the synthesis of zinc selenide thin films by chemical bath deposition. Thin Solid Films, 2020, 693, 137707.	1.8	6
28	A review on the advancements in phosphor-converted light emitting diodes (pc-LEDs): Phosphor synthesis, device fabrication and characterization. Progress in Materials Science, 2020, 109, 100622.	32.8	373
29	Facile control of room temperature nitrogen dioxide gas selectivity induced by copper oxide nanoplatelets. Journal of Colloid and Interface Science, 2020, 560, 755-768.	9.4	26
30	Structural and luminescence properties of Y2O3:Eu3+red phosphor by incorporation of Ga3+ and Bi3+ions. Materials Research Bulletin, 2020, 124, 110752.	5.2	16
31	Preparation and characterization of Ce doped ZnO nanomaterial for photocatalytic and biological applications. Materials Science and Engineering B: Solid-State Materials for Advanced Technology, 2020, 261, 114780.	3.5	41
32	Optical and surface properties of Zn doped CdO nanorods and antimicrobial applications. Colloids and Surfaces A: Physicochemical and Engineering Aspects, 2020, 605, 125369.	4.7	39
33	Photoactive CdO:TiO2 nanocomposites for dyes degradation under visible light. Materials Chemistry and Physics, 2020, 253, 123191.	4.0	17
34	Structural and luminescence properties of thermally stable cool-white light emitting NaCaPO4:Dy3+ phosphor. Optik, 2020, 219, 165026.	2.9	19
35	Red emitting non-rare earth doped LiMgBO3 phosphor for light emitting diodes. Journal of Alloys and Compounds, 2020, 830, 154622.	5.5	12
36	Surface, optical and photocatalytic properties of Rb doped ZnO nanoparticles. Applied Surface Science, 2020, 514, 145930.	6.1	68

#	Article	IF	CITATIONS
37	Luminescence properties of Eu doped ZnO PLD thin films: The effect of oxygen partial pressure. Superlattices and Microstructures, 2020, 139, 106432.	3.1	13
38	Thermally induced structural metamorphosis of ZnO:Rb nanostructures for antibacterial impacts. Colloids and Surfaces B: Biointerfaces, 2020, 188, 110821.	5.0	17
39	Phase transformation on zinc selenide thin films deposited by photo-assisted chemical bath method: The effect of annealing temperature. Materials Science in Semiconductor Processing, 2020, 115, 105118.	4.0	8
40	Optical properties and stability of Bi doped La2O2S. Optical Materials, 2019, 95, 109260.	3.6	10
41	Comparative study of photo- and non-photo-assisted chemical bath deposition of Zinc Selenide thin films using different volumes of hydrazine hydrate. Superlattices and Microstructures, 2019, 134, 106222.	3.1	11
42	Structural, morphological and optical properties of ZnO nanorods grown on a ZnO:Ga seeded thin film: The role of chemical bath deposition precursor concentration at constant and varying II/VI molar ratios. Thin Solid Films, 2019, 687, 137483.	1.8	5
43	(INVITED) Ultraviolet and visible luminescence from bismuth doped materials. Optical Materials: X, 2019, 2, 100025.	0.8	32
44	Improved steady-state photoluminescence derived from the compensation of the charge-imbalance in Ca3Mg3(PO4)4:Eu3+ phosphor. Ceramics International, 2019, 45, 21709-21715.	4.8	34
45	Effects of cationic substitution on the luminescence behavior of Dy3+ doped orthophosphate phosphor. Journal of Alloys and Compounds, 2019, 806, 1127-1137.	5.5	40
46	Photoluminescence and cathodoluminescence of spin coated ZnO films with different concentration of Eu3+ ions. Vacuum, 2019, 169, 108889.	3.5	23
47	Structural and Luminescence Properties of ZnO Nanoparticles Synthesized by Mixture of Fuel Approach in Solution Combustion Method. , 2019, , .		3
48	Multifunction applications of Bi2O3:Eu3+ nanophosphor for red light emission and photocatalytic activity. Applied Surface Science, 2019, 497, 143748.	6.1	32
49	Cathodoluminescence degradation of Bi doped La2O3 and La2O2S phosphor powders. Physica B: Condensed Matter, 2019, 574, 411659.	2.7	10
50	Photoluminescence and thermoluminescence studies of 100â€⁻MeV Si8+ ion irradiated Y2O3:Dy3+ nanophosphor. Journal of Luminescence, 2019, 209, 179-187.	3.1	6
51	Luminescence properties of Bi doped La2O3 powder phosphor. Journal of Luminescence, 2019, 209, 217-224.	3.1	29
52	Analysis of the electron-vibrational interaction in the 5d states of Eu2+ ions in LiSrPO4 host matrix. Journal of Luminescence, 2019, 214, 116564.	3.1	15
53	Controlling the morphology of ZnO NRs grown on GZO seed layer, by use of ethylenediamine and L-cysteine as crystal growth modifiers and complexing agents. Applied Surface Science, 2019, 487, 1198-1208.	6.1	4
54	Structural, optical and photoluminescence properties of Eu doped ZnO thin films prepared by spin coating. Journal of Molecular Structure, 2019, 1192, 105-114.	3.6	32

#	Article	IF	CITATIONS
55	H2S detection capabilities with fibrous-like La-doped ZnO nanostructures: A comparative study on the combined effects of La-doping and post-annealing. Journal of Alloys and Compounds, 2019, 797, 284-301.	5.5	32
56	Facile precipitation synthesis of green-emitting BaY2F8:Yb3+, Ho3+ upconverting phosphor. Ceramics International, 2019, 45, 14205-14213.	4.8	28
57	Influence of Ag, Au and Pd noble metals doping on structural, optical and antimicrobial properties of zinc oxide and titanium dioxide nanomaterials. Heliyon, 2019, 5, e01333.	3.2	47
58	Cathodoluminescence degradation study of the green luminescence of ZnO nanorods. Applied Surface Science, 2019, 484, 105-111.	6.1	14
59	Thermoluminescence response in 60Co gamma rays, 100â€⁻MeV Si8+ and 150â€⁻MeV Au9+ irradiated Y2O3:Ho3 nanophosphor. Journal of Alloys and Compounds, 2019, 778, 554-565.	³⁺ 5.5	9
60	Synthesis and optical studies of KCaVO4:Sm3+/PMMA nanocomposites. Vacuum, 2019, 159, 414-422.	3.5	31
61	Selective detection of CO at room temperature with CuO nanoplatelets sensor for indoor air quality monitoring manifested by crystallinity. Applied Surface Science, 2019, 466, 545-553.	6.1	61
62	Multifunctional properties of plasmonic Cu nanoparticles embedded in a glass matrix and their thermodynamic behavior. Journal of Alloys and Compounds, 2018, 747, 530-542.	5.5	28
63	Self-assembled Cu doped CdS nanostructures on flexible cellulose acetate substrates using low cost sol–gel route. Nano Structures Nano Objects, 2018, 16, 1-8.	3.5	17
64	Effects of octadecylammine molar concentration on the structure, morphology and optical properties of ZnO nanostructure prepared by homogeneous precipitation method. Journal of Luminescence, 2018, 200, 206-215.	3.1	28
65	Enhancement of upconversion emission and temperature sensing of paramagnetic Gd2Mo3O9: Er3+/Yb3+ phosphor via Li+/Mg2+ co-doping. Journal of Alloys and Compounds, 2018, 747, 455-464.	5.5	45
66	Photoluminescence, thermoluminescence and defect centres in Y2O3 and Y2O3:Tb3+ under 100†MeV swift Ni8+ ion beam irradiation. Materials Research Bulletin, 2018, 102, 62-69.	5.2	9
67	Synthesis, structure and optical studies of ZnO:Eu3+,Er3+,Yb3+ thin films: Enhanced up-conversion emission. Colloids and Surfaces A: Physicochemical and Engineering Aspects, 2018, 540, 123-135.	4.7	19
68	In depth study on the notable room-temperature NO2 gas sensor based on CuO nanoplatelets prepared by sonochemical method: Comparison of various bases. Sensors and Actuators B: Chemical, 2018, 266, 761-772.	7.8	69
69	Host sensitized near-infrared emission in Nd 3+ doped different alkaline-sodium-phosphate phosphors. Physica B: Condensed Matter, 2018, 535, 29-34.	2.7	16
70	Upconversion luminescence of Er 3+ /Yb 3+ doped Sr 5 (PO 4) 3 OH phosphor powders. Physica B: Condensed Matter, 2018, 535, 57-62.	2.7	6
71	Structure and photoluminescence properties of Ba 2â^'x Si 4 O 10 :2xSm 3+. Physica B: Condensed Matter, 2018, 535, 50-56.	2.7	3
72	Combustion synthesis and characterization of blue long lasting phosphor CaAl 2 O 4 : Eu 2+ , Dy 3+ and its novel application in latent fingerprint and lip mark detection. Physica B: Condensed Matter, 2018, 535, 149-156.	2.7	40

#	Article	IF	CITATIONS
73	Luminescence properties of Y 2 O 3 :Bi 3+ , Yb 3+ co-doped phosphor for application in solar cells. Physica B: Condensed Matter, 2018, 535, 102-105.	2.7	11
74	Structural and plasmonic properties of noble metal doped ZnO nanomaterials. Physica B: Condensed Matter, 2018, 535, 114-118.	2.7	24
75	Potential of Sm 3+ doped LiSrVO 4 nanophosphor to fill amber gap in LEDs. Physica B: Condensed Matter, 2018, 535, 221-226.	2.7	57
76	A potential green emitting citrate gel synthesized NaSrBO 3 :Tb 3+ phosphor for display application. Physica B: Condensed Matter, 2018, 535, 189-193.	2.7	9
77	Physical and optical properties of lithium borosilicate glasses doped with Dy 3+ ions. Physica B: Condensed Matter, 2018, 535, 194-197.	2.7	18
78	The effect of the host lattice on the optical properties of Bi 3+ in Ca 1-x O:Bi and Ca 1-x (OH) 2 :Bi phosphors. Applied Surface Science, 2018, 433, 155-159.	6.1	5
79	Role of Ga particulates on the structure and optical properties of Y 3 (Al,Ga) 5 O 12 :Tb thin films prepared by PLD. Physica B: Condensed Matter, 2018, 535, 319-322.	2.7	1
80	Influence of Bi doping on the structure and photoluminescence of ZnO phosphor synthesized by the combustion method. Spectrochimica Acta - Part A: Molecular and Biomolecular Spectroscopy, 2018, 190, 164-171.	3.9	44
81	Surface and spectral studies of Sm3+ doped Li4Ca(BO3)2 phosphors for white light emitting diodes. Journal of Alloys and Compounds, 2018, 738, 97-104.	5.5	21
82	Band gap engineering, enhanced morphology and photoluminescence of un-doped, Ga and/or Al-doped ZnO nanoparticles by reflux precipitation method. Journal of Luminescence, 2018, 195, 54-60.	3.1	24
83	Tailoring and optimization of optical properties of CdO thin films for gas sensing applications. Physica B: Condensed Matter, 2018, 535, 314-318.	2.7	33
84	Energy transfer upconversion in Er 3+ -Tm 3+ codoped sodium silicate glass. Physica B: Condensed Matter, 2018, 535, 330-332.	2.7	8
85	Photocatalytic and biological applications of Ag and Au doped ZnO nanomaterial synthesized by combustion. Vacuum, 2018, 157, 508-513.	3.5	73
86	Surface and chemical characterization of ZnO:Eu3+/Yb3+ spin coated thin films using SEM-CL and TOF-SIMS. Vacuum, 2018, 157, 376-383.	3.5	9
87	The effect of pH on the luminescence properties of Y2O3:Bi phosphor powders synthesised using co-precipitation. Vacuum, 2018, 157, 237-242.	3.5	9
88	Synthesis and characterization of Er3+-Yb3+ doped ZnO upconversion nanoparticles for solar cell application. Journal of Alloys and Compounds, 2018, 766, 429-435.	5.5	72
89	Development of an optical thermometry system for phosphor materials. Vacuum, 2018, 155, 702-711.	3.5	6
90	The effect of different annealing temperatures on the structure and luminescence properties of Y 2 O 3 :Bi 3+ thin film fabricated by RF magnetron sputtering. Applied Surface Science, 2017, 424, 407-411.	6.1	14

	· · · · · · · · · · · · · · · · · · ·	TIC SWART		
#	Article		IF	CITATIONS
91	Structural and luminescence properties of Eu3+/Dy3+ embedded sodium silicate glass f emission, lournal of Allovs and Compounds, 2017, 708, 922-931 Colour tuning and energy transfer pathways in MgAl 2 O 4 triply doped with 0.1% Ce 3 x% Tb 3+ <mml:math altimg="sil
overflow=" scroll"="" xmlns:mml="http://www.w3.org/1998/Math/MathML"><mml:mrow><mml:mo< td=""><td>for multicolour }+ , 0.1% Eu 2+ ,</td><td>5.5</td><td>43</td></mml:mo<></mml:mrow></mml:math>	for multicolour }+ , 0.1% Eu 2+ ,	5.5	43
92	overflow="scroll"> <mml:mrow><mml:mo< td=""><td>gn</td><td></td><td></td></mml:mo<></mml:mrow>	gn		

#	Article	IF	CITATIONS
109	Non-plasmonic enhancement of the near band edge luminescence from ZnO using Ag nanoparticles. Journal of Luminescence, 2017, 182, 263-267.	3.1	24
110	Colour tuneable emission from (Y1.995â^'xGax)2O3:Bi3+ phosphor prepared by a sol-gel combustion method. Materials Letters, 2017, 186, 345-348.	2.6	8
111	Transparent conducting ZnO-CdO mixed oxide thin films grown by the sol-gel method. Journal of Colloid and Interface Science, 2017, 487, 378-387.	9.4	50
112	Investigation of thermoluminescence response and trapping parameters of 120ÂMeV Ag9+ and γ-ray exposed NaSrBO3:Dy3+ phosphor for dosimetry. Journal of Alloys and Compounds, 2017, 691, 919-928.	5.5	20
113	Structural and luminescence responses of CaMoO4 nano phosphors synthesized by hydrothermal route to swift heavy ion irradiation: Elemental and spectral stability. Acta Materialia, 2017, 124, 109-119.	7.9	26
114	Structural and optical studies of ZnAl 2 O 4 :x% Cu 2+ <mml:math xmlns:mml="http://www.w3.org/1998/Math/MathML" altimg="si1.gif" overflow="scroll"><mml:mrow><mml:mrow><mml:mo>(</mml:mo><mml:mrow><mml:mn>0</mml:mn><mml: synthesized via citrate sol-gel route. Optical Materials, 2017, 64, 26-32.</mml: </mml:mrow></mml:mrow></mml:mrow></mml:math 	mo ^{3:} < </td <td>18 mml:mo><mr< td=""></mr<></td>	18 mml:mo> <mr< td=""></mr<>
115	Effect of annealing temperature on structural and optical properties of ZnAl 2 O 4 :1.5% Pb 2+ nanocrystals synthesized via sol-gel reaction. Journal of Alloys and Compounds, 2016, 677, 72-79.	5.5	35
116	Spectroscopic studies of Sm3+/Dy3+ co-doped lithium boro-silicate glasses. Journal of Non-Crystalline Solids, 2016, 438, 49-58.	3.1	50
117	Photoluminescence and thermoluminescence properties of Y3(Al,Ga)5O12:Tb3+phosphor. Journal of Modern Optics, 2016, 63, 103-110.	1.3	4
118	Ion-induced modification of structural, optical and luminescence behaviour of Gd2MoO6 nanomaterials: A comparative approach. Vacuum, 2016, 128, 146-157.	3.5	6
119	Role of deposition time on the properties of ZnO:Tb3+ thin films prepared by pulsed laser deposition. Journal of Colloid and Interface Science, 2016, 474, 129-136.	9.4	16
120	Ag7+ ion induced modification of morphology, optical and luminescence behaviour of charge compensated CaMoO4 nanophosphor. Nuclear Instruments & Methods in Physics Research B, 2016, 384, 76-85.	1.4	3
121	Thermoluminescence response of 120 MeV Ag9+ and γ-ray exposed LiMgBO3:Dy3+ nanophosphors for dosimetry. Ceramics International, 2016, 42, 18529-18535.	4.8	11
122	The effect of annealing temperature on the luminescence properties of Y2O3 phosphor powders doped with a high concentration of Bi3+. Journal of Luminescence, 2016, 180, 198-203.	3.1	17
123	Eu 3+ doped down shifting TiO 2 layer for efficient dye-sensitized solar cells. Journal of Colloid and Interface Science, 2016, 484, 24-32.	9.4	44
124	Characterization of annealed Eu 3+ -doped ZnO flower-like morphology synthesized by chemical bath deposition method. Optical Materials, 2016, 60, 294-304.	3.6	39
125	Near infrared quantum cutting of Na + and Eu 2+ -Yb 3+ couple activated SrF 2 crystal. Optical Materials, 2016, 60, 521-525.	3.6	10
126	Embedded plasmonic nanostructures: synthesis, fundamental aspects and their surface enhanced Raman scattering applications. International Reviews in Physical Chemistry, 2016, 35, 353-398.	2.3	58

#	Article	IF	CITATIONS
127	Comparison of Y2O3:Bi3+ phosphor thin films fabricated by the spin coating and radio frequency magnetron techniques. Physica B: Condensed Matter, 2016, 497, 39-44.	2.7	13
128	The effect of different substrate temperatures on the structure and luminescence properties of Y2O3:Bi3+ thin films. Solid State Sciences, 2016, 53, 30-36.	3.2	15
129	Effect of swift heavy ion irradiation on structural, optical and luminescence properties of SrAl2O4:Eu2+, Dy3+ nanophosphor. Radiation Physics and Chemistry, 2016, 122, 48-54.	2.8	10
130	Temperature induced upconversion behaviour of Ho3+-Yb3+ codoped yttrium oxide films prepared by pulsed laser deposition. Journal of Alloys and Compounds, 2016, 672, 190-196.	5.5	20
131	Trap characteristics of UV-activated Y3(Al,Ga)5O12:Ce3+ phosphors. Optik, 2016, 127, 3918-3924.	2.9	9
132	The effect of different annealing temperatures on the structure and luminescence properties of Y2O3:Bi3+ thin films fabricated by spin coating. Applied Surface Science, 2016, 365, 93-98.	6.1	17
133	La 3+ eliminate the blue component from the emission of Y 2 O 3 : Bi 3+. Materials Letters, 2016, 171, 171-173.	2.6	2
134	Structural and optical characterization of mechanically milled Mg-TiO2 and nitrided Mg-TiO -N nanostructures: Possible candidates for gas sensing application. Applied Surface Science, 2016, 360, 1047-1058.	6.1	3
135	Structural, surface and luminescence properties of Ca3B2O6:Dy3+ phosphors. Ceramics International, 2016, 42, 5743-5753.	4.8	35
136	Electrical and optical properties of p-type codoped ZnO thin films prepared by spin coating technique. Physica E: Low-Dimensional Systems and Nanostructures, 2016, 77, 1-6.	2.7	34
137	Structural and luminescence properties of SrAl2O4:Eu2+,Dy3+,Nd3+ phosphor thin films grown by pulsed laser deposition. Physica B: Condensed Matter, 2016, 480, 116-124.	2.7	8
138	The influence of substrate temperature and deposition pressure on pulsed laser deposited thin films of CaS:Eu2+ phosphors. Physica B: Condensed Matter, 2016, 480, 186-190.	2.7	9
139	Characterization of crystallite morphology for doped strontium fluoride nanophosphors by TEM and XRD. Physica B: Condensed Matter, 2016, 480, 169-173.	2.7	12
140	Surface characterization of ZnO nanorods grown by chemical bath deposition. Physica B: Condensed Matter, 2016, 480, 42-47.	2.7	10
141	NaSrVO4:Sm3+ â^ An n-UV convertible phosphor to fill the quantum efficiency gap for LED applications. Ceramics International, 2016, 42, 2317-2323.	4.8	29
142	Spectroscopic properties of Pr3+ ions embedded in lithium borate glasses. Physica B: Condensed Matter, 2016, 480, 111-115.	2.7	39
143	Effect of doping concentration on the conductivity and optical properties of p-type ZnO thin films. Physica B: Condensed Matter, 2016, 480, 31-35.	2.7	19
144	Dopant distribution and influence of sonication temperature on the pure red light emission of mixed oxide phosphor for solid state lighting. Ultrasonics Sonochemistry, 2016, 28, 79-89.	8.2	24

#	Article	lF	CITATIONS
145	The influence of laser wavelength on the structure, morphology, and photoluminescence properties of pulsed laser deposited CaS: Eu2+thin films. Journal of Modern Optics, 2015, 62, 1102-1109.	1.3	4
146	P-type conductivity in doped and codoped ZnO thin films synthesized by RF magnetron sputtering. Journal of Modern Optics, 2015, 62, 1368-1373.	1.3	25
147	Concentration quenching, surface and spectral analyses of SrF2:Pr3+ prepared by different synthesis techniques. Optical Materials, 2015, 42, 204-209.	3.6	21
148	Noble metal nanoparticles embedding into polymeric materials: From fundamentals to applications. Advances in Colloid and Interface Science, 2015, 226, 187-202.	14.7	89
149	Luminescent properties, intensity degradation and X-ray photoelectron spectroscopy analysis of CaS:Eu2+ powder. Optical Materials, 2015, 40, 68-75.	3.6	32
150	Effects of Cr3+ mol% on the structure and optical properties of the ZnAl2O4:Cr3+ nanocrystals synthesized using sol–gel process. Ceramics International, 2015, 41, 6776-6783.	4.8	60
151	X-ray photoelectron spectroscopy and luminescent properties of Y2O3:Bi3+ phosphor. Applied Surface Science, 2015, 332, 198-204.	6.1	45
152	Characteristics of the mechanical milling on the room temperature ferromagnetism and sensing properties of TiO2 nanoparticles. Applied Surface Science, 2015, 331, 362-372.	6.1	42
153	A near-UV-converted LiMgBO3:Dy3+ nanophosphor: Surface and spectral investigations. Applied Surface Science, 2015, 329, 40-46.	6.1	53
154	The role of oxygen and titanium related defects on the emission of TiO2:Tb3+ nano-phosphor for blue lighting applications. Optical Materials, 2015, 46, 510-516.	3.6	52
155	Radiative energy transfer in ZnAl2O4:0.1% Ce3+, x% Eu3+ nanophosphor synthesized by sol–gel process. Physica B: Condensed Matter, 2015, 468-469, 11-20.	2.7	19
156	Thermoluminescence of calcium phosphate co-doped with gadolinium and praseodymium. Radiation Measurements, 2015, 77, 26-33.	1.4	18
157	The influence of Ag9+ ion irradiation on the structural, optical and luminescence properties of Sm3+ doped NaSrBO3: Stability of color emission. Nuclear Instruments & Methods in Physics Research B, 2015, 351, 27-34.	1.4	9
158	Persistent photoluminescence emission from SrTa2O6:Pr3+ phosphor prepared at different temperatures. Ceramics International, 2015, 41, 8828-8836.	4.8	17
159	Comparison and analysis of Eu3+ luminescence in Y3Al5O12 and Y3Ga5O12 hosts material for red lighting phosphor. Materials Chemistry and Physics, 2015, 166, 167-175.	4.0	33
160	Luminescence of Alternating SiO2:Tb and SiO2:Ce Thin Films Produced by Sol-gel Spin Coating. Materials Today: Proceedings, 2015, 2, 4111-4117.	1.8	3
161	Effect of alkali metal ions (Li+, Na+ and K+) on the luminescence properties of CaMgB2O5: Sm3+ nanophosphor. Nano Structures Nano Objects, 2015, 3, 9-16.	3.5	40
162	A study on the sensing of NO2 and O2 utilizing ZnO films grown by aerosol spray pyrolysis. Materials Chemistry and Physics, 2015, 162, 628-639.	4.0	20

#	Article	IF	CITATIONS
163	Review of rare earth activated blue emission phosphors prepared by combustion synthesis. Renewable and Sustainable Energy Reviews, 2015, 52, 596-612.	16.4	76
164	Luminescence and electron degradation properties of Bi doped CaO phosphor. Applied Surface Science, 2015, 356, 1064-1069.	6.1	14
165	Optical and Chemical Properties of Alq3:PMMA Blended Thin Films. Materials Today: Proceedings, 2015, 2, 4019-4027.	1.8	11
166	Upconversion based temperature sensing ability of Er3+–Yb3+codoped SrWO4: An optical heating phosphor. Sensors and Actuators B: Chemical, 2015, 209, 352-358.	7.8	355
167	CaTiO3:Eu3+, a potential red long lasting phosphor: Energy migration and characterization of trap level distribution. Journal of Alloys and Compounds, 2015, 622, 1068-1073.	5.5	41
168	Effect of Eu doping on the photoluminescence properties of ZnO nanophosphors for red emission applications. Applied Surface Science, 2014, 308, 419-430.	6.1	105
169	The greenish-blue emission and thermoluminescent properties of CaTa2O6:Pr3+. Journal of Alloys and Compounds, 2014, 589, 88-93.	5.5	33
170	A comparative study of the effect of Ni9+ and Au8+ ion beams on the properties of poly(methacrylic) Tj ETQq0 C	0 rgBT /C	overlock 10 Tf
171	Dependence of luminescence properties of CaTiO3:Pr3+ on different TiO2 polymorphs. Powder Technology, 2014, 256, 477-481.	4.2	10
172	Effect of different annealing temperatures on the optical properties of Y3(Al,Ga)5O12:Tb thin films grown by PLD. Physica B: Condensed Matter, 2014, 439, 77-82.	2.7	9
173	Structural and morphology analysis of annealed Y3(Al,Ca)5O12:Tb thin films synthesized by pulsed laser deposition. Applied Surface Science, 2014, 305, 732-739.	6.1	10
174	Effect of annealing on the structural, morphological and photoluminescence properties of ZnO thin films prepared by spin coating. Journal of Colloid and Interface Science, 2014, 428, 8-15.	9.4	107
175	Defect-induced magnetism in undoped and Mn-doped wide band gap zinc oxide grown by aerosol spray pyrolysis. Applied Surface Science, 2014, 311, 14-26.	6.1	43
176	Temperature-dependence on the structural, optical, and paramagnetic properties of ZnO nanostructures. Applied Surface Science, 2014, 293, 62-70.	6.1	82
177	Spectral and surface investigations on Eu3+ doped K3Y(PO4)2 nanophosphor: A promising orange–red phosphor for white light-emitting diodes. Optical Materials, 2014, 36, 996-1001.	3.6	25
178	Roles of doping ions in afterglow properties of blue CaAl2O4:Eu2+,Nd3+ phosphors. Physica B: Condensed Matter, 2014, 439, 153-159.	2.7	42
179	Photoluminescence properties of Ce3+-doped SrAl2O4 prepared using the solution combustion method. Physica B: Condensed Matter, 2014, 439, 177-180.	2.7	26
180	Luminescence of Ce doped MgAl2O4 prepared by the combustion method. Physica B: Condensed Matter, 2014, 439, 109-114.	2.7	52

#	Article	IF	CITATIONS
181	Effect of Eu3+ on the structure, morphology and optical properties of flower-like ZnO synthesized using chemical bath deposition. Journal of Luminescence, 2014, 147, 85-89.	3.1	62
182	Generation of white-light from Dy3+ doped Sr2SiO4 phosphor. Physica B: Condensed Matter, 2014, 439, 126-129.	2.7	60
183	Synthesis and characterization of Y2O3:Eu3+ phosphors using the Sol-Combustion method. Physica B: Condensed Matter, 2014, 439, 181-184.	2.7	13
184	The effects of Eu-concentrations on the luminescent properties of SrF 2 :Eu nanophosphor. Journal of Luminescence, 2014, 156, 150-156.	3.1	39
185	Properties of flower-like ZnO nanostructures synthesized using the chemical bath deposition. Materials Science in Semiconductor Processing, 2014, 27, 33-40.	4.0	37
186	Tunable and white emission from ZnO:Tb3+ nanophosphors for solid state lighting applications. Chemical Engineering Journal, 2014, 255, 541-552.	12.7	146
187	A comparative investigation on ion impact parameters and TL response of Y2O3:Tb3+ nanophosphor exposed to swift heavy ions for space dosimetry. Journal of Alloys and Compounds, 2014, 589, 5-18.	5.5	34
188	Role of swift heavy ions irradiation on the emission of boron doped ZnO thin films for near white light application. Journal of Alloys and Compounds, 2014, 594, 32-38.	5.5	32
189	Enhanced upconversion and temperature sensing study of Er3+–Yb3+ codoped tungsten–tellurite glass. Sensors and Actuators B: Chemical, 2014, 202, 1305-1312.	7.8	152
190	Influence of ultrasonication times on the tunable colour emission of ZnO nanophosphors for lighting applications. Ultrasonics Sonochemistry, 2014, 21, 1549-1556.	8.2	63
191	Luminescent properties and quenching effects of Pr3+ co-doping in SiO2:Tb3+/Eu3+ nanophosphors. Optical Materials, 2014, 36, 732-739.	3.6	11
192	Enhanced exciton emission from ZnO nano-phosphor induced by Yb3+ ions. Materials Letters, 2014, 119, 71-74.	2.6	33
193	Swift heavy ion irradiation induced modification in structural, optical and luminescence properties of Y2O3:Tb3+ nanophosphor. Journal of Luminescence, 2014, 146, 162-173.	3.1	62
194	Enhanced UVB emission and analysis of chemical states of Ca5(PO4)3OH:Gd3+,Pr3+ phosphor prepared by co-precipitation. Journal of Physics and Chemistry of Solids, 2014, 75, 998-1003.	4.0	58
195	Improvement of the photoluminescent intensity of ZnTa2O6:Pr3+ phosphor. Materials Research Bulletin, 2014, 55, 150-155.	5.2	8
196	Compound Luminescent Semiconductors: Their Properties and Uses. , 2013, , 73-86.		1
197	Photoluminescence and thermoluminescence properties of Pr3+ doped ZnTa2O6 phosphor. Powder Technology, 2013, 247, 147-150.	4.2	30
198	Origin of the red emission in zinc oxide nanophosphors. Materials Letters, 2013, 101, 57-60.	2.6	255

#	Article	IF	CITATIONS
199	Role of film thickness on the properties of ZnO thin films grown by sol-gel method. Thin Solid Films, 2013, 539, 161-165.	1.8	152
200	Afterglow enhancement with In3+ codoping in CaTiO3:Pr3+ red phosphor. Powder Technology, 2013, 237, 141-146.	4.2	72
201	Conversion of Y3(Al,Ga)5O12:Tb3+ to Y2Si2O7:Tb3+ thin film by annealing at higher temperatures. Applied Surface Science, 2013, 270, 331-339.	6.1	30
202	The effect of Ce3+ on structure, morphology and optical properties of flower-like ZnO synthesized using the chemical bath method. Journal of Luminescence, 2013, 143, 463-468.	3.1	37
203	Improved luminescence properties of pulsed laser deposited Y3(Al,Ga)5O12:Tb thin films by post deposition annealing. Journal of Luminescence, 2013, 143, 201-206.	3.1	16
204	Effect of Br+6 ions on the structural, morphological and luminescent properties of ZnO/Si thin films. Applied Surface Science, 2013, 279, 472-478.	6.1	68
205	Synthesis, spectral and surface investigation of NaSrBO3: Sm3+ phosphor for full color down conversion in LEDs. Journal of Alloys and Compounds, 2013, 554, 214-220.	5.5	84
206	Cathodoluminescent stability of rare earth tantalate phosphors. Journal of Luminescence, 2013, 140, 14-20.	3.1	19
207	Thermo-luminescence kinetic parameters of γ-irradiated Sr ₄ Al ₁₄ O ₂₅ :Eu ²⁺ , Dy ³⁺ phosphors. Radiation Effects and Defects in Solids, 2013, 168, 1022-1029.	1.2	4
208	Surface state of Y3(Al,Ga)5O12:Tb phosphor under electron beam bombardment. Applied Surface Science, 2012, 258, 6495-6503.	6.1	36
209	The cathodoluminescence degradation and surface characterization of β-Ca3(PO4)2:Tb phosphor. Optical Materials, 2012, 34, 1398-1405.	3.6	20
210	A comparative study on structural, morphological and luminescence characteristics of Zn3(VO4)2 phosphor prepared via hydrothermal and citrate-gel combustion routes. Physica B: Condensed Matter, 2012, 407, 1485-1488.	2.7	52
211	Lattice site dependent cathodoluminescence behavior and surface chemical changes in a Sr5(PO4)3F host. Physica B: Condensed Matter, 2012, 407, 1505-1508.	2.7	12
212	Surface chemical changes of CaTiO3:Pr3+ upon electron beam irradiation. Physica B: Condensed Matter, 2012, 407, 1517-1520.	2.7	16
213	Luminescence studies of a combustion-synthesized blue–green BaAlxOy:Eu2+,Dy3+ nanoparticles. Physica B: Condensed Matter, 2012, 407, 1561-1565.	2.7	12
214	Luminescence from Ce in sol–gel SiO2. Physica B: Condensed Matter, 2012, 407, 1595-1598.	2.7	11
215	Synthesis and characterization of BaAl2O4:Eu2+ co-doped with different rare earth ions. Physica B: Condensed Matter, 2012, 407, 1603-1606.	2.7	46
216	Sensitizing effects of ZnO quantum dots on red-emitting Pr3+-doped SiO2 phosphor. Physica B: Condensed Matter, 2012, 407, 1607-1610.	2.7	12

#	Article	IF	CITATIONS
217	Investigation of ageing characteristics and identification of surface chemical changes on SrGa2S4:Ce3+ display phosphor under electron beam bombardment. Physica B: Condensed Matter, 2012, 407, 1645-1648.	2.7	2
218	Surface characterization and luminescent properties of SrAl2O4:Eu2+, Dy3+ nano thin films. Physica B: Condensed Matter, 2012, 407, 1660-1663.	2.7	13
219	PL and CL degradation and characteristics of SrAl2O4: Eu2+,Dy3+ phosphors. Physica B: Condensed Matter, 2012, 407, 1664-1667.	2.7	27
220	Phosphorescent and thermoluminescent properties of SrAl2O4:Eu2+, Dy3+ phosphors prepared by solid state reaction method. Physica B: Condensed Matter, 2012, 407, 1679-1682.	2.7	36
221	Low voltage electron induced cathodoluminescence degradation and surface characterization of Sr3(PO4)2:Tb phosphor. Applied Surface Science, 2011, 257, 10147-10155.	6.1	36
222	Dependence of Eu3+ luminescence dynamics on the structure of the combustion synthesized Sr5(PO4)3F host. Journal of Alloys and Compounds, 2011, 509, 2544-2551.	5.5	31
223	Effects of Ce3+ concentration, beam voltage and current on the cathodoluminescence intensity of SiO2:Pr3+–Ce3+ nanophosphor. Journal of Alloys and Compounds, 2011, 509, 2986-2992.	5.5	10
224	Luminescent properties and X-ray photoelectron spectroscopy study of ZnAl2O4:Ce3+,Tb3+ phosphor. Journal of Alloys and Compounds, 2011, 509, 10115-10120.	5.5	93
225	Investigations on the low voltage cathodoluminescence stability and surface chemical behaviour using Auger and X-ray photoelectron spectroscopy on LiSrBO3:Sm3+ phosphor. Materials Research Bulletin, 2011, 46, 987-994.	5.2	50
226	Luminescence response and CL degradation of combustion synthesized spherical SiO2:Ce nanophosphor. Materials Research Bulletin, 2011, 46, 2359-2366.	5.2	11
227	Luminescence investigations on LiAl5O8:Tb3+ nanocrystalline phosphors. Current Applied Physics, 2011, 11, 341-345.	2.4	35
228	Characterization of luminescent and thermal properties of long afterglow SrAlxOy:Eu ²⁺ ,Dy ³⁺ phosphor synthesized by combustion method. Polymer Composites, 2011, 32, 219-226.	4.6	13
229	Luminescence characterization and electron beam induced chemical changes on the surface of ZnAl2O4:Mn nanocrystalline phosphor. Applied Surface Science, 2011, 257, 3298-3306.	6.1	33
230	The effect of different gas atmospheres on luminescent properties of pulsed laser ablated SrAl2O4:Eu2+,Dy3+ thinfilms. Journal of Luminescence, 2011, 131, 119-125.	3.1	22
231	Synthesis and characterization of Ce3+ doped silica (SiO2) nanoparticles. Journal of Luminescence, 2011, 131, 1249-1254.	3.1	46
232	Electron beam induced green luminescence and degradation study of CaS:Ce nanocrystalline phosphors for FED applications. Applied Surface Science, 2010, 256, 1720-1724.	6.1	8
233	Auger electron/X-ray photoelectron and cathodoluminescent spectroscopic studies of pulsed laser ablated SrAl2O4:Eu2+,Dy3+ thin films. Applied Surface Science, 2010, 257, 512-517.	6.1	18
234	Luminescence investigations of Ce3+ doped CaS nanophosphors. Journal of Alloys and Compounds, 2010, 492, L8-L12.	5.5	47

#	Article	IF	CITATIONS
235	Combustion synthesis and luminescence investigation of Na3Al2(PO4)3:RE (RE = Ce3+, Eu3+ and Mn2+) phosphor. Journal of Alloys and Compounds, 2010, 492, 384-388.	5.5	102
236	Luminescent properties of Ca0.97Al2O4:Eu0.012+,Dy0.023+ phosphors prepared by combustion method at different initiating temperatures. Journal of Alloys and Compounds, 2010, 508, 262-265.	5.5	27
237	Photon emission mechanisms of different phosphors. Nuclear Instruments & Methods in Physics Research B, 2009, 267, 2630-2633.	1.4	12
238	Characteristic properties of Y2SiO5:Ce thin films grown with PLD. Physica B: Condensed Matter, 2009, 404, 4431-4435.	2.7	6
239	Photoluminescence and phosphorescence properties of MAl2O4:Eu2+, Dy3+ (M=Ca, Ba, Sr) phosphors prepared at an initiating combustion temperature of 500°C. Physica B: Condensed Matter, 2009, 404, 4440-4444.	2.7	83
240	Characterization and luminescent properties of SiO2:ZnS:Mn2+ and ZnS:Mn2+ nanophosphors synthesized by a sol–gel method. Physica B: Condensed Matter, 2009, 404, 4470-4475.	2.7	35
241	The effect of Mg2+ ions on the photoluminescence of Ce3+-doped silica. Physica B: Condensed Matter, 2009, 404, 4499-4503.	2.7	20
242	Structural, luminescent and thermal properties of blue SrAl2O4:Eu2+, Dy3+ phosphor filled low-density polyethylene composites. Physica B: Condensed Matter, 2009, 404, 4504-4508.	2.7	13
243	Resolution of Eu2+ asymmetrical emission peak of SrAl2O4:Eu2+, Dy3+ phosphor by cathodoluminescence measurements. Materials Letters, 2008, 62, 3192-3194.	2.6	47
244	Degradation of Y2SiO5:Ce phosphor powders. Journal of Luminescence, 2007, 126, 37-42.	3.1	20
245	Effects of SnO2 surface coating on the degradation of ZnS thin film phosphor. Applied Surface Science, 2007, 253, 8513-8516.	6.1	16
246	Characterization of Y2SiO5:Ce thin films. Optical Materials, 2007, 29, 1338-1343.	3.6	16
247	Enhanced luminescence and degradation of SiO2:Ce,Tb powder phosphors prepared by a sol–gel process. Journal of Physics and Chemistry of Solids, 2006, 67, 1749-1753.	4.0	50
248	A comparative study between the simulated and measured cathodoluminescence generated in ZnS:Cu, Al, Au phosphor powder. Journal of Luminescence, 2005, 113, 191-198.	3.1	10
249	Degradation of ZnS:Cu,Al,Au phosphor powder in different gas mixtures. Journal of Luminescence, 2004, 109, 93-102.	3.1	15
250	Extracting inter-diffusion parameters of TiC from AES depth profiles. Applied Surface Science, 2003, 205, 231-239.	6.1	27
251	Effect of a CdO coating on the degradation of a ZnS thin film phosphor material. Applied Surface Science, 2002, 187, 137-144.	6.1	20
252	Low temperature effect on the electron beam induced degradation of ZnS:Cu,Al,Au phosphor powders. Applied Surface Science, 2002, 193, 77-82.	6.1	9

#	Article	IF	CITATIONS
253	Modelling the effect of a thin ZnO layer on the cathodoluminescence generated in ZnS phosphor powders. Thin Solid Films, 2002, 408, 260-269.	1.8	9
254	ZnS thin films grown on Si(100) by XeCl pulsed laser ablation. Applied Surface Science, 2001, 177, 73-77.	6.1	41
255	Electron beam induced degradation of a pulsed laser deposited ZnS:Cu,Au,Al thin film on a Si(1 0 0) substrate. Applied Surface Science, 2001, 183, 304-310.	6.1	32
256	The oxidation of industrial FeCrMo steel. Corrosion Science, 2000, 42, 1725-1740.	6.6	74
257	The influence of sulphur segregation on the oxidation of industrial FeCrMo steel. Corrosion Science, 2000, 42, 991-1004.	6.6	12
258	Electron beam-induced degradation of zinc sulfide-based phosphors. Surface Science, 2000, 451, 174-181.	1.9	28
259	The difference in degradation behaviour of ZnS:Cu,Al,Au and ZnS:Ag,Cl phosphor powders. Applied Surface Science, 1999, 140, 63-69.	6.1	51
260	Electron Beam Degradation of Sulfide-Based Thin-Film Phosphors for Field Emission Flat Panel Displays. Materials Research Society Symposia Proceedings, 1998, 508, 261.	0.1	5
261	ZnS:Cu,Al,Au phosphor degradation under electron excitation. Applied Surface Science, 1997, 120, 9-14.	6.1	68